Assessing the tumour microenvironment with DCE-MRI and DCE-Ultrasound

F. Moosvi[1,2], P. Bevan[3], C. Bailey[1,2], and G. Stanisz[1,2]
[1]Imaging Physics, Sunnybrook Health Sciences Centre, Toronto, Ontario, Canada, [2]Medical Biophysics, University of Toronto, Toronto, Ontario, Canada, [3]McMaster University, Hamilton, Ontario, Canada

Introduction

The use of complementary non-invasive imaging modalities has been proposed to track disease progression, particularly cancer [1], while simultaneously evaluating therapeutic efficacy. The applicability of these techniques spans a wide spectrum of disease processes, but a major obstacle is a limited ability to compare parameters obtained from different modalities, especially those from exogenous contrast agents or tracers. Standard imaging techniques can determine tumour location and morphology as well as dynamic characteristics of contrast agent uptake. For instance, parameters derived from dynamic contrast enhanced MRI (DCE-MRI) can provide information about the tumour microenvironment (e.g., volume transfer constant K^{TRANS} and extra-cellular volume fraction v_E). On the other hand, intravascular microbubbles used in DCE-ultrasound can provide highly specific information about the tumour vasculature (e.g., relative blood volume rBV, and blood flow rBF) [1,2]. We hypothesize that using DCE-MRI in combination with DCE-US will extend non-invasive characterization of tumours and facilitate a more complete analysis of the tumour microenvironment during treatment. Challenges such as radically different image contrast and acquisition mechanisms between MRI and US have stifled advancement in this field. We propose to bypass a number of issues with a novel imaging protocol with *a priori* image co-registration between MR and US data, accurate to within 0.5mm in-plane and 1mm through-plane.

Materials and Methods

Apparatus: A physical co-registration apparatus was designed to enable co-planar MR and US imaging of immobilized rats. Acoustic waves transmitted from a transducer located above the apparatus were coupled to a water tank placed between the rat and the transducer. A 1-mm thin staircase-shaped insert - visible in both MR and US (Fig. 1) - was fixed in the water tank and provided a reference plane for *a priori* image co-registration. A custom surface coil was built in to the apparatus.

Animals: Six immunocompromised rats (Hsd:RH-Foxn1 *rnu*) had human breast cancer cells (MDA-MB231) implanted subcutaneously in the hind leg. The xenografts were allowed to grow until the longest tumour diameter was approximately 1cm (~ 4-6 weeks). Rats were imaged at baseline, treated with 8Gy radiation immediately afterwards and imaged again 24h and 48h post radiation. Prior to each imaging session, rats were anaesthetized with isofluorane and lain prone on the co-registration apparatus with the tumour flush against the acoustically transparent membrane coupling the tumour to the water tank.

MRI: Imaging was performed using a 3T scanner (GE Signa, Milwaukee) with a custom-built surface coil and a 3D f-SPGR protocol with TR/TE= 4.0/2.1 ms and voxel size of 0.39 x 0.39 x 2.0 mm. The DCE-MR data was acquired at a temporal resolution of 10.4s following a bolus of gadodiamide (Omniscan, GE Healthcare; ~120 µL, dose of 0.39 mmol•kg^{-1}). Central tumour slices were selected for pixel-by-pixel analysis and the initial area under the curve (IAUC) for the first 300 seconds was calculated and normalized to the IAUC value in a muscle ROI.

Ultrasound: US imaging was performed using the Vevo2100 scanner (VisualSonics; Toronto, Canada) operating at a centre frequency of 12.5 MHz and a FOV of 32mm x 36 mm. The staircase insert was used to align the US transducer at the same reference plane as MRI, and anatomical slices were acquired axially 1.0 mm apart. DCE-US data was acquired using the non-linear imaging protocol at a temporal resolution of 0.2s for a duration of 100-200s following a bolus of microbubbles (~140µL, MicroMarker; VisualSonics). The Vevo2100 system software was used to draw ROIs around the tumour boundary and quantify the bulk tumour signal enhancement over time, normalized to the muscle enhancement.

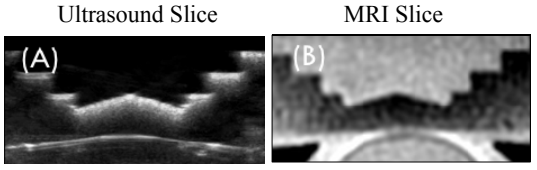

Figure 1. A fixed 1-mm thick fiducial marker (stair-case shaped) is placed in the water tank, designed to be visible in both US (A) and MRI (B). The fiducial marker serves as a common reference point and ensures co-planar imaging through-plane within 1mm.

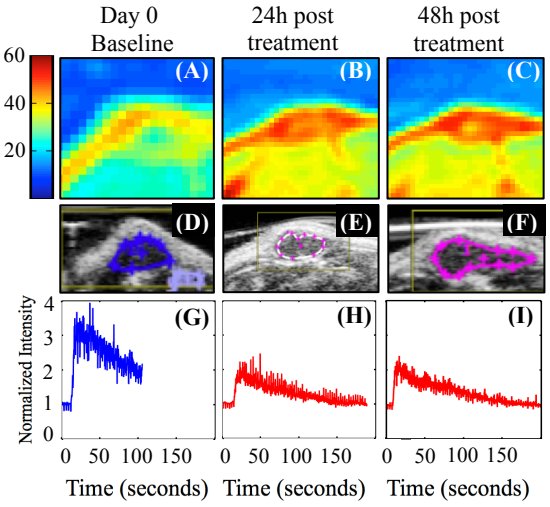

Figure 2. (A) Pre-treatment baseline DCE-MRI data has been shown as a normalized (to pre-bolus tissue signal) IAUC parameter map of the tumour region scaled from no enhancement (blue) to maximum enhancement (red). Parameter maps for the same tumour 24h (B) and 48h (C) post treatment indicate a measurable change in IAUC. Ultrasound images of the same tumour with ROIs drawn are shown in (D,E,F). Signal enhancement from microbubbles peaks higher and decays much faster pre-treatment (G) than 24h (H) and 48h (I) post treatment.

Results and Discussion

Analysed data from a representative rat is shown in Fig. 2. There was a marked increase in IAUC values compared to baseline both 24h (Fig. 2B) and 48h (Fig. 2C) post treatment. Radiation induced apoptosis, necrosis and vascular disruption likely caused a drastic change in the tumour microenvironment post treatment. The MR contrast agent extravasates from disrupted blood vessels and has access to the increased extravascular extracellular space, ultimately leading to the increased IAUC. Imaging the same tumour plane with DCE-US, a different trend is noted: following treatment, both the peak signal intensity as well as the washout/decay rate decreases post-treatment (Fig. 2H,I). Microbubbles are typically between 2-10µm in diameter and have been confirmed to be intravascular [3]. As expected, disruption of the tumour microvasculature restricts the flow of microbubbles through the tumour leading to a net decrease in bubbles and thus, decreased signal enhancement post treatment.

References

[1] Laking, G.R. et al., *Critical Reviews in Oncology Hematology*, 2006. **58** (2): 95-113.
[2] Burns, P.N. et al., *Ultrasound Quarterly* ,2006. **22** (1): 5-13.
[3] Ellegala, D et al., *Circulation*, 2003. **108** (1): 336-341